Automated High-Performance, High-Temperature Combustion Total Organic Carbon Analyzer

ARTICLE *in* ANALYTICAL CHEMISTRY · SEPTEMBER 1996

Impact Factor: 5.64 · DOI: 10.1021/ac960370z

2 AUTHORS, INCLUDING:

Kenneth Mopper
Old Dominion University
147 PUBLICATIONS **9,368** CITATIONS

SEE PROFILE

Anal. Chem. **1996,** *68,* 3090−3097

Automated High-Performance, High-Temperature Combustion Total Organic Carbon Analyzer

Jianguo Qian† and Kenneth Mopper*

Department of Chemistry, Washington State University, Pullman, Washington 99164

A high-temperature combustion (HTC) total organic carbon analyzer, which has significant design improvements over existing systems, was developed. The new injection system directly connects a loop-type autoinjector to the head of the HTC column. This connection facilitates the coupling of an autosampler to the injection system. The entire injection process is closed to the atmosphere, thereby improving the precision and eliminating potential contamination during injection. Injections can be made every 3−5 min, depending on the injection and inorganic carbon sparging modes used. The HTC column was designed without a "cold" zone or dead space at the top. These improvements eliminated the memory (or carry-over) effect, which is a potential problem in some HTC column designs. The HTC column is packed with pure quartz beads instead of a relatively expensive Pt-based catalyst, without loss in the oxidation efficiency, as indicated by 100% recovery for various compounds with different refractory properties and by intercomparison with Pt-based HTC systems. The precision for seawater is ∼±0.6% (RSD) at the 80 μM C level. Typically, greater than 5000 injections of seawater can be made without significant deterioration of column performance. The effects of column temperature and carrier gas flow rate on the oxidation efficiency, sensitivity, and reproducibility are reported. Finally, evidence is presented that suggests that there is a relationship between the refractory nature of pure compounds and the peak width. This potential relationship may be a useful tool for quantifying the refractory nature of organic carbon in natural waters.

Various techniques have been employed to determine the concentration of dissolved organic carbon (DOC) or total organic carbon (TOC, if unfiltered) in fresh and seawaters. These techniques include wet chemical oxidation,[1,2] photooxidation,[3] dry combustion,[4] sealed tube combustion,[5,6] and high-temperature combustion (HTC).[7] A form of HTC, high-temperature catalytic oxidation, which usually employs a platinum-based (Pt-based) catalyst to facilitate oxidation,[8] has become the method of choice for the analysis of TOC and DOC in seawater and other natural waters because this method appears to have a greater oxidation efficiency than most of the other methods.[9,10] Consequently, a large number of HTC systems have been built, and several commercial instruments are currently available.[11−15]

Even though HTC appears to have a greater oxidation efficiency than other techniques, some HTC instrumental designs have problems that can give rise to poor reproducibility and poor accuracy. Poor reproducibility and poor accuracy can also arise from contamination during sampling, sample manipulations (e.g., transfers, filtration, and acidification), incomplete sparging of inorganic carbon, and sample storage.[12,16−18] However, in this paper, we focus on the instrumental problems. The latter are mainly related to the sample injection system, memory (or carry-over) effects, system blank evaluation, and motion sensitivity. These problems are particularly evident in the analysis of seawater. As a result of the high salt content and the low DOC concentration, ∼40 μM (0.5 ppm) in deep water and 80−90 μM (∼1 ppm) in surface waters, the accurate, precise, and artifact-free determination of DOC in seawater has been a major instrumental challenge despite over 30 years of effort.[17] The necessity for accurate and precise determination DOC in natural waters has increased sharply over the last few years because several large-scale models and major field studies of marine systems have focused on carbon cycling and its relation to global fluxes, climatic fluctuations, and food web dynamics. This need has been partly met through recent concerted efforts of the marine community, which involved several workshops and intercomparisons.[19,20] Although the precision (and presumably the accuracy) of DOC analyses of seawater has improved markedly as a result of these efforts, maintaining this high precision is still difficult and labor intensive, especially at sea. Most shipboard TOC analyses are currently being performed by manual injection, often requiring two or three operators working in shifts. Although attempts have been made to use unmodified commercial instruments at sea, their perfor-

† Present address: MQ Scientific, Inc., P.O. Box 2435, Pullman, WA 99165-2435.

(1) Duursma, E. K. *Neth. J. Sea Res.* **1961**, *1*, 1−148.
(2) Menzel, D. W.; Vaccaro, R. F. *Limnol. Oceanogr.* **1964**, *9*, 138−142.
(3) Armstrong, F. A. J.; Williams, P. M.; Strickland, J. D. H. *Nature* **1966**, *221*, 481−483.
(4) Skopintsev, B. A. *Mar. Hydrophys. Inst.* **1960**, *19*, 1−14.
(5) Fry, B.; Saupe, S.; Hullar, M.; Peterson, B. J. *Mar. Chem.* **1993**, *41*, 187−193.
(6) Alperin, M. J.; Martens, C. S. *Mar. Chem.* **1993**, *41*, 135−143.
(7) Sharp, J. H. *Mar. Chem.* **1973**, *1*, 211−229.
(8) Sugimura, Y.; Suzuki, Y. *Mar. Chem.* **1988**, *24*, 105−131.
(9) Sharp, J. H.; Suzuki, Y.; Munday, W. L. *Mar. Chem.* **1993**, *41*, 253−259.
(10) Koprivnjak, J.-F.; Blanchette, J. G.; Bourbonniere, R. A.; Clair, T. A. *Water Res.* **1995**, *29* (1), 91−94.
(11) Tanoue, E. *Earth Planet. Sci. Lett.* **1992**, *111*, 201−216.
(12) Peltzer, E. T.; Brewer, P. G. *Mar. Chem.* **1993**, *41*, 243−252.
(13) Martin, W. R.; McCorkle, D. C. *Limnol. Oceanogr.* **1993**, *38*, 1464−1479.
(14) Chen, W.; Wangersky, P. J. *Mar. Chem.* **1993**, *41*, 167−171.
(15) Cauwet, G. *Mar. Chem.* **1994**, *47*, 55−64.
(16) Sharp, J. H.; Peltzer, E. T.; Alperin, M. J.; Cauwet, G.; Farrington, J. W.; Fry, B.; Karl, D. M.; Martin, J. H.; Spitzy, A.; Tugrul, S.; Carlson, C. A. *Mar. Chem.* **1993**, *41*, 37−49.
(17) Wangersky, P. J. *Mar. Chem.* **1993**, *41*, 61−74.
(18) Tupas, L. M.; Popp, B. N.; Karl, D. M. *Mar. Chem.* **1994**, *45*, 207−216.
(19) Hedges, J. I.; Farrington, J. *Mar. Chem.* **1993**, *41*, 5−10.
(20) Sharp, J. H.; Benner, R.; Bennet, L.; Carlson, C. A.; Fitzwater, S. E.; Peltzer, E. T.; Tupas, L. *Mar. Chem.* **1995**, *48*, 91−108.

S0003-2700(96)00370-8 CCC: $12.00

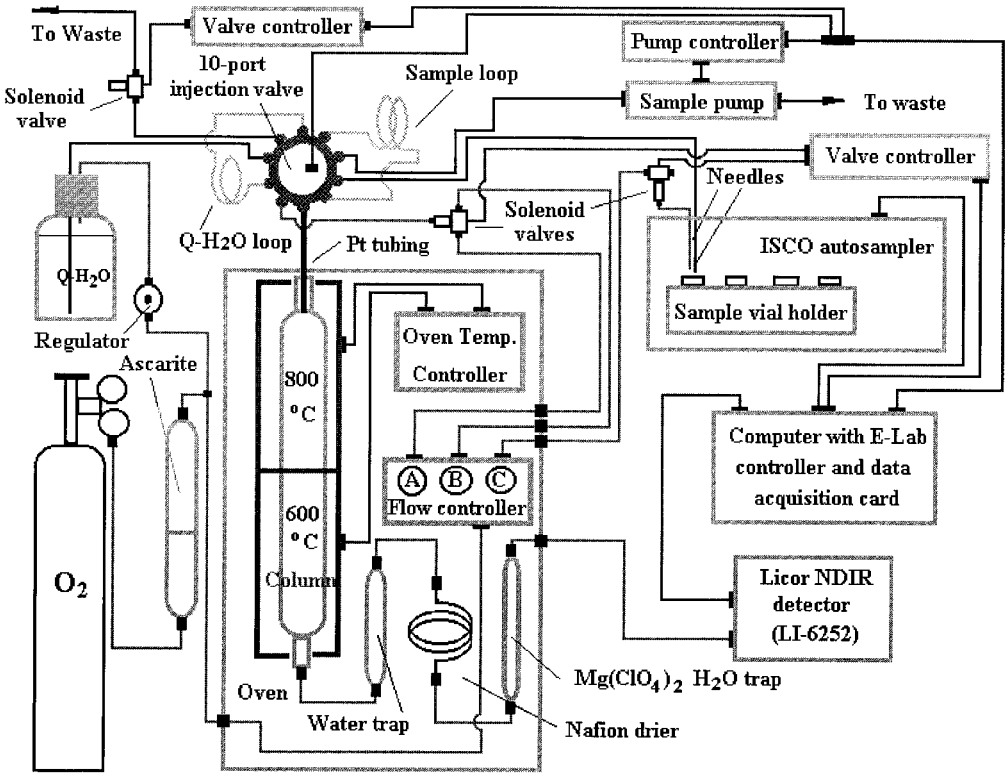

Figure 1. Schematic of the high-performance, high-temperature combustion TOC/DOC analyzer. Flow controller notation: (A) carrier gas, (B) injection gas, and (C) sample sparging gas.

mance was generally too unstable for routine, automated analysis of seawater samples, in part due to motion/vibration sensitivity.

Seawater samples can also present problems for the injection systems of TOC analyzers. Sample injection problems may arise from both valve movement and syringe injection because many systems use either a sliding metallic valve, which is susceptible to salt abrasion, or a septumless injection port for manual sample injection. The use of these semi-open systems can result in a major disturbance in the gas flow and an increased potential for contamination (e.g., from a contaminated needle). For these types of manual injection systems, obtaining good precision often depends on the skill level of the operator. In addition to these problems, the high salt content of seawater can cause mechanical and clogging problems with autosampler/injector components of some fully automated TOC instruments.

Memory effects may arise because some HTC column designs have a "cold" zone at the top, where vaporized organic carbon (OC) together with salts can deposit on the wall. During subsequent injections, these deposits may wash off or "flake off" randomly and become oxidized, giving rise to memory effects.[21] These effects are difficult to eliminate and may adversely affect the reproducibility and accuracy.

Accuracy is also strongly dependent on evaluation of the system blank, which in turn is dependent on conditioning of the instrument, especially the column. Column conditioning is often accomplished with repeated injections of water. Hundreds, even thousands of injections may be required to obtain a low and stable blank for some types of Pt-based HTC columns, which is problematic using manual injection.[22,23] In addition, variations in the injection delay interval (i.e., the time between injections) can result in blank variability and consequently in poor precision and accuracy.[21]

Most HTC columns use Pt-based catalysts, supposedly to ensure complete oxidation of organic carbon to CO_2. However, these columns are relatively expensive, and the catalytic sites may be subject to poisoning or deactivation by salt deposition.[21,24] It is not clear what function, if any, the catalyst plays in the oxidation process.[21,23,24]

In order to overcome these difficulties, we have constructed an HTC system with major improvements in the injection system and column design. We have succeeded in coupling a loop autoinjector directly to the HTC column so that the entire injection process is closed to the atmosphere, thereby improving the precision and eliminating contamination during injection. We have greatly decreased the dead volume at the top of the column, and since the sample injection takes place entirely within the column's "hot" zone, memory effects have been virtually eliminated. Also, the new column design allowed us to use inexpensive quartz beads instead of Pt-based catalysts without loss of oxidation efficiency.

EXPERIMENTAL SECTION

Instrumentation. Details of our HTC TOC/DOC analyzer and columns are shown in Figures 1 and 2, respectively. The main operation principles are similar to those of previously described HTC TOC analyzers.[7,8,11,12] Organic carbon is converted to CO_2 by HTC, and after removal of water vapor, the CO_2 produced is determined by nondispersive IR, Li-Cor Model LI-6252 (Lincoln, NE). The Li-Cor detector was chosen because of its proven insensitivity to motion and vibration. The two-stage

(21) Perdue, E. M.; Mantoura, F. *Mar. Chem.* **1993**, *41*, 51−60.
(22) Benner, R.; Strom M. *Mar. Chem.* **1993**, *41*, 153−160.
(23) Skoog, A.; Thomas, D.; Lara, R. *Mar. Chem.*, in press.
(24) Bauer, J. E.; Ocelli, M. L.; Williams, P. M.; McCaslin, P. C. *Mar. Chem.* **1993**, *41*, 75−89.

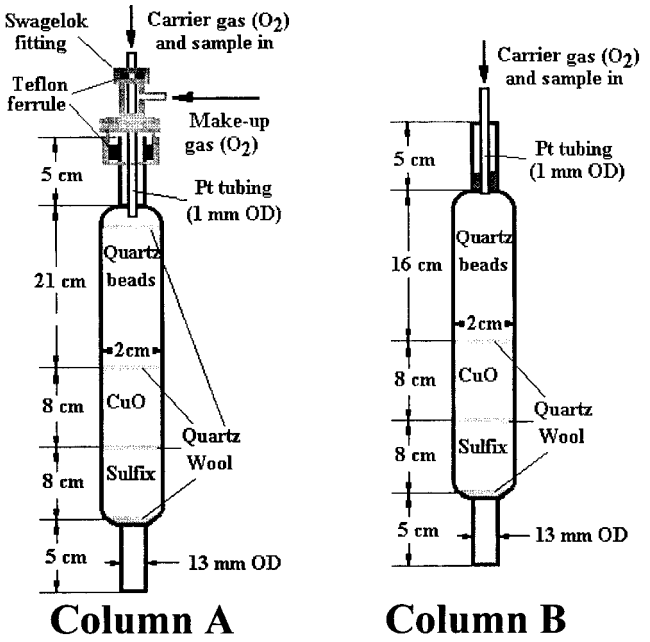

Figure 2. Schematics of the TOC/DOC combustion columns: (A) with a cold zone and make-up gas and (B) without a cold zone and no make-up gas.

combustion oven (Figure 1) was fabricated in-house, with each stage independently controlled by a Model CN76000 temperature controller (Omega Engineering, Stamford, CT). The latter has a precision of ±0.25% at 800 °C. Sample injection is achieved by a 10-port injection valve (Valco Instruments, Houston, TX) and an ISCO autosampler (Model ISIS, ISCO, Lincoln NE). The autosampler vials (4 mL) are borosilica glass and are sealed with screw caps lined with silicon rubber-backed Teflon septa (National Scientific, Lawrenceville, CA). The carrier gas flow rate is controlled by a 0−60 psi regulator (Model 6014; Amicon, Beverly, MA). Instrument control, including sample sparging and injection, and peak area integration are performed with an E-Lab controller board (OMS Tech, Miami, FL) mounted in an IBM-clone 386 computer. Switching of gas lines is controlled by three-way solenoid valves coupled to a Valve Driver II (General Valve, Fairfield, NJ), which in turn is connected to the E-Lab board for sequencing. These valves were modified by replacing the internal rubber O-rings with custom made Teflon O-rings. Postcolumn water vapor is removed using a custom-built glass condenser, followed by a Nafion drier tubing (MD-110-48F, Perma Pure, Toms River, NJ), and finally a magnesium perchlorate trap.

During the injection of a sample, the sequence of events is as follows: the sample is sparged of inorganic carbon with ultrahigh purity oxygen (60 mL/min) for 5 min and then drawn into the sample loop by the transfer pump (Figure 1). Low-carbon deionized water (DI water) is loaded into a DI water loop by a "gas pump" simultaneously as the sample is loaded. After the sample and DI water loadings are complete, the 10-port injection valve is switched to the inject position. At this time, the three-way valve controlling the injection gas (~400 mL/min) and carrier gas (usually 120−130 mL/min) is switched to the injection gas position for 2 s and then returned to the normal operating condition (carrier gas open, injection gas closed). The 10-port valve is configured so that the sample first goes into the column followed immediately by the DI water plug. The analysis time is 5 min per injection (two injections/vial) when the autosparging mode is used. The analysis time can be cut down to ~2.5 min for repeated injection of a single sample, since autosparging is not needed. A commercial version of the automated TOC/DOC instrument is available through MQ Scientific (Pullman, WA).

Column Packing Materials and Reagents. Column packing materials include an upper bed of cylindrical quartz beads, 2 × 2 mm or 3 × 3 mm (Quartz Sci., Fairport Harbor, OH), and lower beds of copper oxide (14−24 mesh) and Sulfix (8−20 mesh), both from Wako Chemicals USA (Richmond, VA). All reagents were used as received. The purities (given as percentages in parentheses) were those stated by the manufacturer on the reagent bottle for the particular lot number. Antipyrine (98%), phosphoric acid (H_3PO_4, 85 wt %, 99.999% purity), phthalic acid (99.5%), magnesium perchlorate, thiourea (99+%), and sulfathiazole (98%) were all ACS reagent grade (Aldrich, Milwaukee, WI). Caffeine (99%) and glyoxal termeric dihydrate (GTD) (98%) were obtained from Sigma (St. Louis, MO). EDTA (100.1%) was obtained from Fisher Scientific (Pittsburgh, PA). Methanol was HPLC grade (Burdick & Jackson, Baxter, McGaw Park, IL). Anhydrone was purchased from J. T. Baker (Phillipsburg, NJ). Ultrahigh purity oxygen (Liquid Air Corp., Walnut Creek, CA) was used for sample sparging and as the carrier, make-up, and injection gas. All standard solutions were prepared in DI water obtained from a Nanopure system with a UV organic oxidation attachment (Barnstead, Pittsburgh, PA) and 0.2-μm filtered seawater (see below). The carbon content of the DI water is estimated to be less than 2 μM C (E. T. Peltzer, personal communication). Samples and standards were acidified to a pH of ~2 with phosphoric acid prior to sparging. Sample acidification was performed by adding 10 μL of 20% H_3PO_4 (v/v) to 3.2 mL of sample in the autosampler vial. The final pH was ≤2.4 for samples and standards (as measured by a pH meter). The 20% H_3PO_4 solution was prepared by diluting 85 wt % H_3PO_4 with DI water.

Seawater Sample. The seawater sample used in the various optimization tests was collected from the upper 10 m at a site in the confluence of the Weddell and Scotia Seas, near 60°S and 50°W in October 1993. The site was located within a highly productive biomass front ~100 km north of the ice edge and was characterized by a well-mixed surface layer and a sharp pycnocline at ~120 m. The sample was collected using a Niskin bottle attached to a CTD rosette. Once on board, the sample was immediately filtered through 5.0- and 0.2-μm polypropylene filters (Polypure TDC Capsules, Gelman) that were attached directly to the Niskin bottle. The sample was stored in refrigerated at 2 °C in a fluorinated polypropylene jerry can (Cole Parmer, Niles, IL) until analyzed in the home laboratory. The sample had a DOC concentration of 85 μM C, which is between that reported by Skoog[25] for the Weddell Sea and that reported by Dafner[26] for the productive Polar Front Zone.

Column Design and Memory Effects. Two column designs were developed in attempts to meet the requirements of a loop-type sample injection (Figure 2). These requirements were that the sample injection be performed in a closed system and that the sample be directly, completely, and quickly injected into the high-temperature zone of the combustion column. The column A design contains a relatively large dead volume (~8 cm^3) at the top. Thus, the head of the column was continuously swept by a

(25) Skoog, A. Ph.D. Thesis, University of Gothenburg, Gothenburg, Sweden, 1995.
(26) Dafner, E. V. *Mar. Chem.* **1992**, *37*, 275−283.

make-up gas (O_2) to minimize band broadening. For the column A design, the sample loop was 100 μL; the carrier gas flow rate was ~120 mL/min. The make-up gas flow rate was ~30 mL/min. Unfortunately, the column A design did not meet all the stated requirements, since the top of the column contains a "cold" zone, which was found to give rise to memory, or sample carry-over, effects (see below). Thus, in order to eliminate these effects, a non-cold zone column (column B) was designed in which the sample is injected directly into the high-temperature zone of the column. In addition, the column B design does not contain a dead volume at the top; thus, a make-up gas flow was not used. For column B, the sample loop was 60 or 80 μL; the DI water wash loop was 30 μL. The flow rate of the carrier gas was ~130 mL/min, except during sample injection when it was increased to ~400 mL/min for 2 s. Tests of the memory effect were performed by alternately injecting low-carbon DI water, seawater, and a high-carbon standard.

Column Oxidation Efficiency. Standard compounds with different refractory properties were used to determine the oxidation efficiency as a function of column temperature and carrier gas flow rate. These compounds have been previously used to test the recoveries of high-temperature catalytic[5,8] and other oxidation methods.[27−28] The compounds were dissolved in DI water and seawater at concentrations of 100, 300, and 400 μM C.

RESULTS AND DISCUSSION

Coupling the Autoinjector to the HTC Column. Several problems were encountered when we first attempted to connect a loop-type autoinjector to the HTC column. After only a few hundred injections of seawaters, the tubing that connected the injection valve to the column became partially clogged. As a consequence, the sample in the loop could not be transferred quickly to the column, resulting in considerable tailing and poor precision. Similar sample transfer problems were noted in a previous attempt at coupling a loop injector to a HTC column.[14] To prevent clogging and improve the reproducibility, the sample in the loop must be transferred rapidly to the column during injection. Consequently, the instrument was programmed to deliver a high flow of carrier gas (~400 mL/min, 2 s) at the time of injection. In addition, a small amount of DI water (e.g., 30 μL) was automatically injected simultaneously with (i.e., immediately after) each sample injection to keep salt deposits from building up in the connecting tubing. The DI water injection also helped reduce memory effects (see below) and increase the lifetime of the autoinjection valve.

Initially, stainless steel or titanium tubing was used to connect the autoinjector to the HTC column. The lifetimes of these tubes were short (several days) because they were easily oxidized at high temperature. To solve this problem, we tested Pt tubing and found that, as long as tube was held in a static position, its lifetime was much greater than the column lifetime.

Memory Effects. When the column A design was used, memory or carry-over effects were encountered. These effects were particularly evident when injections of seawater, or high OC standards, were followed by injections of DI water. Figure 3a shows that the peak area of the first injection of DI water was always larger than the following replicate injections. In addition

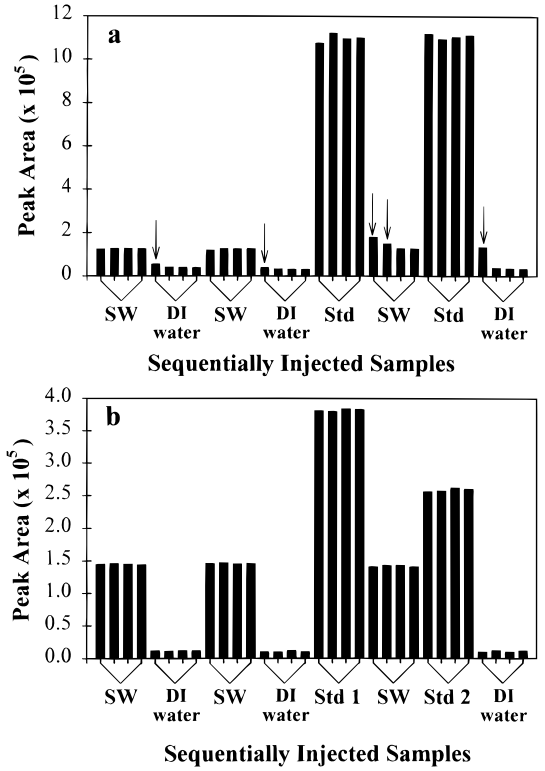

Figure 3. Memory effect tests. (a) Column A (see Figure 2): The column temperature was 800 °C; carrier gas flow rate, 150 mL/min. The arrows indicate sample "carry-over" problems. Notation: SW, Antarctic seawater; Std, 400 μM C phthalic acid in DI water. (b) Column B (see Figure 2): The column temperature was 750 °C; carrier gas flow rate, 130 mL/min. Notation: SW, Antarctic seawater; Std 1, 300 μM C phthalic acid in DI water; Std 2, 100 μM C phthalic acid in SW.

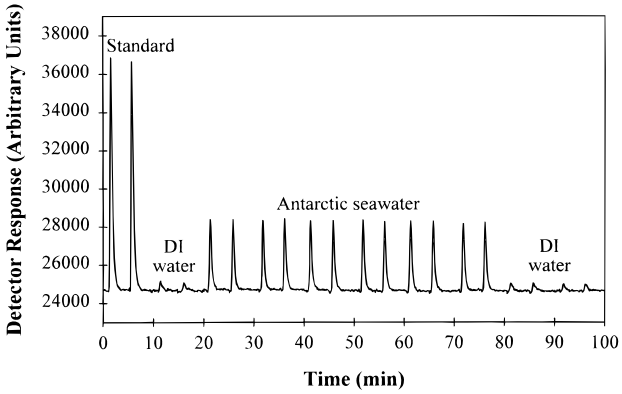

Figure 4. Typical raw results using the Li-Cor NDIR detector and column B. The standard used was sulfathiazole (300 μM C). Experimental conditions: upper column temperature, 800 °C; lower column temperature, 600 °C; carrier gas flow rate, 133 mL/min.

to this carry-over effect, during the injection of seawater, an unusually large peak appeared randomly. The latter problem may have resulted from the deposition and flaking off of OC in the cold zone of column A.[21]

Due to the random nature of the memory effects, especially the flaking off of uncombusted OC in the cold zone, it is difficult or impossible to correct for them since they may affect standards and samples differently. Discarding unexpectedly small or large peaks will improve the precision, but this may have a negative impact on the accuracy, especially if the large peaks are due to residual OC deposits from prior samples. Thus, the overall impact

(27) Gershey, R. M.; MacKinnon, M. D.; Williams, P. J.; Moore, R. M. *Mar. Chem.* **1979**, *7*, 289−306.
(28) Walsh, T. W. *Mar. Chem.* **1989**, *26*, 295−311.

Table 1. Oxidation Efficiency as a Function of the Column Temperature[a]

	column B					column A	
compounds	800/600[b]	750/600[b]	650/600[b]	800/650[b]	average[c]	750/600[b]	640/600[b]
antipyrine	98.76	98.98	100.58	101.63	99.99 ± 1.36	nd[d]	nd
caffeine	102.93	101.80	102.08	104.23	102.76 ± 1.06	nd	nd
EDTA	99.99	99.30	99.01	100.28	99.65 ± 0.59	99.50	65.52
GTD[e]	103.72	nd	103.68	102.78	103.39 ± 0.51	nd	nd
phthalate	99.24	99.20	99.24	101.51	99.80 ± 1.14	99.93	84.33
sulfathiazole	100.31	101.07	100.58	100.75	100.68 ± 0.32	nd	nd
thiourea	102.74	102.91	103.44	103.10	103.05 ± 0.29	nd	nd
					100.76 ± 0.38		
average[f]	100.96 ± 1.86	100.36 ± 1.56	101.20 ± 1.73	100.53 ± 1.56		99.81 ± 0.27	83.17 ± 20.56
seawater (μM)	84.77 ± 0.81	84.27 ± 0.73	84.94 ± 1.11	84.59 ± 0.97	84.65 ± 0.34	nd	nd

[a] The efficiencies were calculated as percent relative to methanol, assuming it is oxidized 100% at 640−800 °C. The carrier gas flow rate was 130 mL/min for column B and 150 mL/min for column A. The calculated concentration of all compounds was 300 μM C. Each data point represents an average of four replicate injections (average RSD ± 0.9%). [b] Upper column temperature (°C)/lower column temperature (°C). [c] Average recovery of the same compound run at the different oven temperature settings. Note: RSDs are given instead of standard errors. [d] nd = no data. [e] Glyoxal termeric dihydrate. [f] Average recovery of all compounds run at the same oven temperature settings. Note: RSDs are given instead of standard errors.

may be lowered recoveries. To completely eliminate memory effects, a non-cold zone column was developed (column B; Figure 2). With this column design, no memory effects were observed for alternating injections of seawater, standards, and DI water (Figure 3b), indicating that there was no buildup of OC at the top of the column between injections. Figure 4 shows typical raw data for sequential injections of a 300 μM C standard and an 85 μM C Antarctic seawater sample followed by injections of DI water (using column B). At least 5000 injections of seawater can be made with no significant effect on peak shape or column performance, which is in agreement with other investigators.[23]

Effect of Temperature on Oxidation Efficiency. In both columns A and B, pure quartz beads were used as the packing materials instead of a Pt-based catalyst. We chose quartz because previous studies suggested that it produced a lower blank and that it was at least as effective as Pt-based packings in oxidizing OC.[21,29] Our results indicate that, for the column B design (non-cold zone), the oxidation efficiency for various compounds was independent of column temperature between 640 and 800 °C, within the analytical precision (Table 1). The recoveries for all tested compounds were taken relative to methanol, which was assumed to be oxidized at 100% efficiency over the tested temperature range (RSD for methanol over this range was ±0.77%; see Precision, Accuracy, Detection Limit, Calibration, and Blank section below). The average recovery for all compounds was ~100% (actually 100.76 ± 0.38% RSD) and ranged from 99.65% for EDTA to 103.39% for GTD. The average relative standard deviation ranged between 0.29 and 1.36% over the different column temperature settings. The average recoveries for caffeine, GTD, and thiourea were somewhat higher than 100% (~103%), which was probably caused by carbon-rich impurities in those standards. Interestingly, the high recovery of thiourea for all temperatures contrasts with the previously reported recovery of about 82−94% for the Pt-catalyzed sealed tube HTC method.[5] The Antarctic seawater yielded an average concentration of 84.65 μM C with a RSD of 0.34% over the different column temperatures (average of four injections at each temperature setting) (Table 1). The above results indicate that a catalytic packing material is not necessary for obtaining a 100% recovery. The non-cold zone column (column B) packed with pure quartz beads yielded 100% recovery for all tested compounds, as well as for seawater (see below).

In contrast, the recoveries for column A, which contains a cold zone at the top, were strongly dependent on column temperature (Table 1). At 750 °C, the recoveries were nearly 100%, but at 640 °C, the recoveries were only 84.3 and 65.5% for phthalic acid and EDTA, respectively. The low recoveries were probably due to the memory effect, which should become worse with decreasing column temperature. Unoxidized EDTA and phthalic acid were probably deposited on the wall of the cold zone, resulting in low recoveries at 640 °C. EDTA appears to be somewhat harder to oxidize than phthalic acid (see Peak Width section), thus explaining its somewhat lower recovery.

Effects of Carrier Gas Flow Rate. The optimal flow rate range is mainly determined by the oxidation efficiency of the column (i.e., the column temperature) and the system dead volume (column, water traps, postcolumn gas driers, CO_2 detector cell). Typically, flow rates of 100−200 mL/min are used.

Using the non-cold zone column (column B, Figure 2), the effect of flow rate on the oxidation efficiency was examined (Table 2). Approximately 100% recovery was obtained for all tested standard compounds at 170 and 130 mL/min (assuming 100% recovery for methanol at both flow rates). Also, the seawater sample yielded the same concentration at both flow rates. These results indicate that the oxidation efficiency at 800 °C was not affected by flow rates up 170 mL/min. Higher flow rates were not examined.

In contrast, the carrier gas flow rate affected the sensitivity, i.e., the slope of the calibration curve. A plot of flow rate vs slope of the calibration curve yields a linear relationship with a slope of −0.000 073 mL/min (Figure 5). The negative slope implies a lower sensitivity at the higher flow rate. The decrease in sensitivity with increasing flow rate could be related to a decrease in oxidation efficiency due to the shorter residence time in the column or to a change in the response of the CO_2 detector. However, we found that the oxidation efficiency was not affected by the flow rate (see previous section) or by changes in the response time of Li-Cor detector from 5 to 1 s. The slope change appears to be due to the different residence times of the sample

(29) Williams, P. M.; Bauer, J. E.; Robertson, K. J.; Wolgast, D. M.; Occelli, M. L. *Mar. Chem.* **1993**, *41*, 271−281.

Table 2. Oxidation Efficiency as a Function of the Flow Rate[a]

compounds	130 mL/min[b]	170 mL/min[b]	average[c]
antipyrine	98.76	100.55	99.66 ± 1.23
caffeine	102.93	103.17	103.05 ± 0.16
EDTA	99.99	99.95	99.97 ± 0.03
GTD[d]	103.72	103.42	103.58 ± 0.20
phthalate	99.24	100.02	99.63 ± 0.55
sulfathiazole	100.31	99.34	99.83 ± 0.69
thiourea	102.74	103.41	103.08 ± 0.46
			101.10 ± 0.19
average[e]	100.96 ± 1.86	101.23 ± 1.75	
seawater (μM)	84.77 ± 0.81	83.65 ± 1.79	84.22 ± 0.95

[a] In this experiment, a non-cold zone column (column B) was employed, and the column temperature was constant (upper, 800 °C; lower, 600 °C). The concentration of the test compounds was 300 μM C. The efficiencies were calculated as percent relative to methanol by assuming it is oxidized at 100% at both flow rates. Each data point represents an average of four replicate injections (average RSD ± 0.9%). [b] Flow rate of carrier gas. [c] Average recovery of the same compound run at the different flow rates. Note: RSDs are given instead of standard errors. [d] Glyoxal termeric dihydrate. [e] Average recovery of all compounds run at the same flow rates. Note: RSDs are given instead of standard errors.

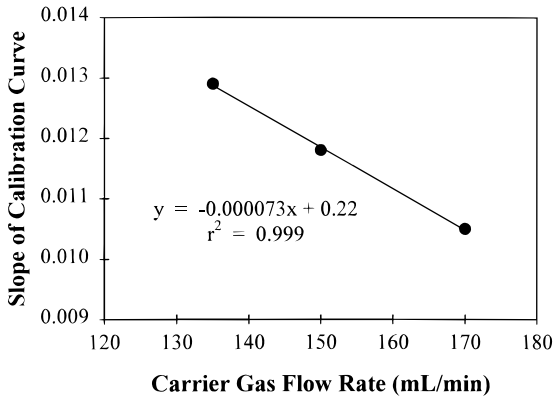

Figure 5. Relationship between the flow rate of the carrier gas and the slope of the calibration curve using column B.

CO_2 plug in the detector cell at the different flow rates. The lower sensitivity at the higher flow rate implies that slight flow fluctuations will have a more detrimental impact on the precision at the higher flow rate than at the lower one. Thus, a variation in the flow rate of 2% at 130 and 170 mL/min will cause a change in the slope of the calibration curve by 1.5 and 2.6%, respectively. This effect will translate into a larger RSD at the higher flow rate. For example, at a flow rate of 130 mL/min, the RSD for the Antarctic seawater sample (n = 4) was ±0.81%, while a somewhat larger RSD, ±1.79%, was obtained at 170 mL/min (Table 2). It should be pointed out that the better precision at the lower flow rate is somewhat offset by peak broadening, which may adversely affect the integration precision. Because the sensitivity is flow rate dependent, a high precision (e.g., <±1% at 50 μM C) requires a very stable gas flow. Several possibilities for increasing the stability of the flow, especially during sample injection, are currently being explored.

Injection Delay Time. The injection delay time is the time period between injections, while the sequential injection time is the total time elapsed for a set of injections. Figure 6 shows the effects of injection delay time and sequential injection time on the system blank. A plot of the blank vs injection delay time yields

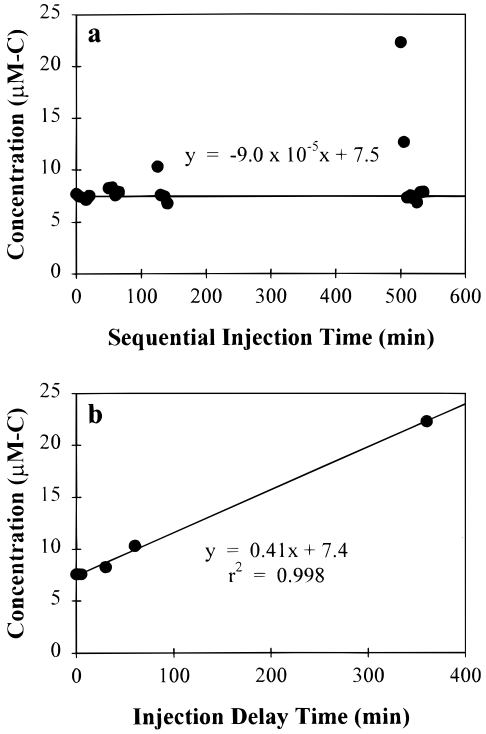

Figure 6. Column blank as a function of sequential injection time (a) and injection delay time (b). The column was conditioned with hundreds of injections of DI water prior to the start of the experiment. Experimental conditions: column B; sample, DI water; upper column temperature, 750 °C; lower column temperature, 600 °C; carrier gas flow rate, 140 mL/min.

a slope of 0.041 μM C/min (Figure 6b). Thus, if the delay time was 1 h, the system blank would increase 2.5 μM C for the first injection after the delay. After the first or second injection, the blank returns to a stable, low value (Figure 6a). These results indicate that a variable injection delay period adversely affects the precision. The reason for this effect is not known;[21] however, this problem can be minimized with the use of an autosampler/autoinjector that employs a short and reproducible injection delay time, e.g., 5 min. Our TOC analyzer also uses an autosparging gas system which has a constant sample sparging time. Consequently, any minor organic contamination that might be present in the sparging gas would be incorporated within the blank.[21]

Precision, Accuracy, Detection Limit, Calibration, and Blank. From the above, it is apparent that the precision is affected by various factors including variations in carrier gas flow rate and column temperature, the presence or absence of a cold zone at the head of the column, memory effects, contamination during injection, variable injection delay time, and possibly sample sparging time.[12,21] We found that most of these variables are eliminated or minimized by using a closed autoinjection/autosparging system coupled with the non-cold zone, low dead volume combustion column (Figure 2B). The RSD for replicate injections of the Antarctic seawater sample was ±0.64% (n = 12) at the 85 μM C level (Figure 4). The RSD for a 50 μM C standard in DI water was ±1.09% (n = 4), while that of DI water was ±4.0% (n = 4) at ~7 μM C level (including the system blank).

The accuracy was determined by using methanol in DI water as a standard at 650−800 °C and assuming 100% oxidation efficiency, which is reasonable given its high volatility and combustibility. In support of this assumption, compounds with much higher refractory natures[5,27,28] yielded average recoveries

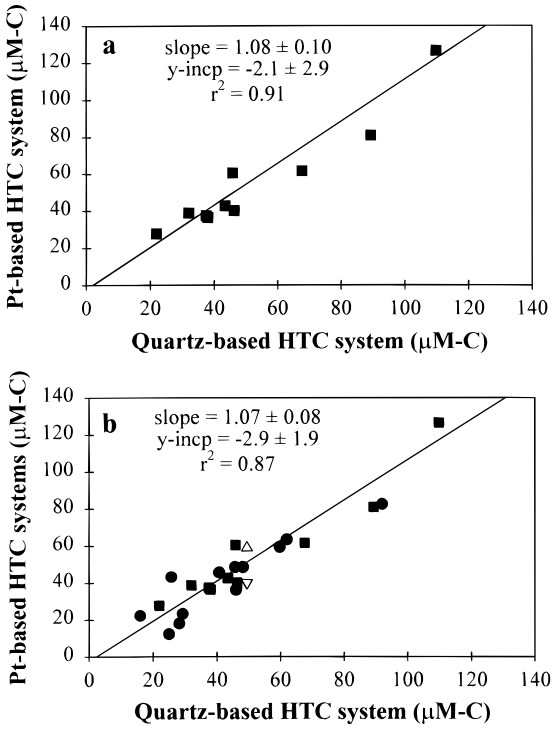

Figure 7. DOC intercomparison between a Pt-based HTC with manual injection[30] and a quartz-based HTC system with autoinjection system:[30] (a) Replicate aliquots of ultrafiltered seawater samples (integrated permeates, solid squares) from different CFF systems analyzed by both HTC analyzers. (b) Data from part a and nonidentical permeate samples (solid circles) from CFF systems close to a concentration factor of 2. Open triangle (down) is 0.2-μm filtered seawater sample,[30] open triangle (up) is 0.2-μm filtered seawater sample. Note that the slopes = 1, indicating 100% oxidation efficiency.

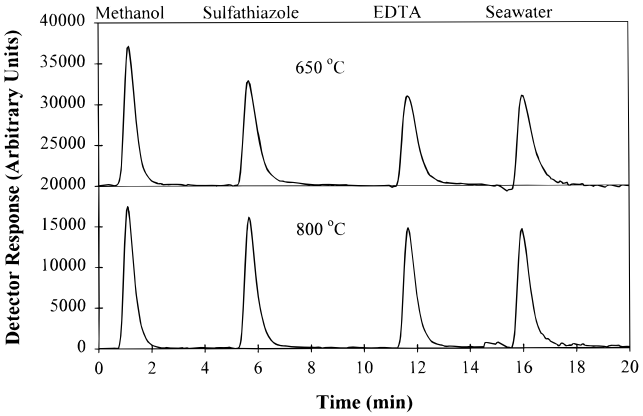

Figure 8. Effect of upper column temperature on peak broadening of different compounds. Experimental conditions: column B; flow rate, 135 mL/min; concentration of standards, 300 μM C. The DOC concentration of seawater was normalized to 300 μM C to facilitate comparison to the test compounds.

Table 3. Effect of Column Temperature on the Peak Width of Different Compounds (Arbitrary Units)

	column temp[b]		
compounds	650/600	750/600	800/600
methanol	2.94	2.88	2.83
antipyrine	3.18	2.73	3.04
caffeine	3.22	2.75	2.87
thiourea	3.39	2.97	2.89
phthalate	3.47	3.11	3.04
sulfathiazole	3.68	3.11	3.10
EDTA	4.18	3.24	3.09
seawater	4.33	3.81	3.20

[a] Experimental conditions: column B (see Figure 2); injection volume, 110 μL; carrier gas flow rate, 135 mL/min. [b] Upper column temperature (°C)/lower column temperature (°C).

of ~100% at all combustion temperatures and flow rates tested using column B (Tables 1 and 2). In addition, an intercomparison experiment with a manual injection, Pt-based HTC system gave excellent agreement, as shown in Figure 7. The DOC intercomparison was run in conjunction with an intercomparison of cross-flow filtration (CFF) techniques using open ocean seawater off Hawaii.[30] In Figure 7a, replicate aliquots of ultrafiltered seawater samples (integrated permeates) from different CFF systems were analyzed at random by both systems. The slope and *y*-intercept of the regression line using Pearson's major axis[31] are essentially 1 and 0, respectively. Similar results were obtained when the data set was expanded to include non-identical permeate samples that were collected from the CFF systems at slightly different times during the CFF process (close to a concentration factor of 2). The latter results (Figure 7b) gave a slightly poorer correlation, mainly due to the somewhat greater scatter at the lower DOC concentrations. The 1:1 correlation further supports that 100% oxidation efficiency was achieved by the quartz HTC column, assuming that Pt-based catalytic HTC systems achieve 100% oxidation efficiency.[21,24]

The detection limit (S/N = 3) was about 2−3 μM C with a 60-μL sample loop, a column temperature of ≥750 °C, and a flow rate of ≤140 mL/min. The detection limit is strongly dependent on the size of the sample loop, column temperature (temperatures less than ~750 °C result in peak broadening), and gas flow rate (see section on Effects of Carrier Gas Flow Rate).

Calibration was carried out using either phthalic acid or sulfathiazole dissolved in seawater or DI water. The calibration curve was linear (r^2 > 0.999; n = 10) for concentrations between 20 and 500 μM C. Higher concentrations were not examined.

A newly packed, quartz bead column requires only ~100 injections of DI water at 800 °C to reduce the total blank (system + DI water) to less than 10 μM C. Normally, for a well-conditioned column (after a few hundred injections), this blank drops to ~7 μM C. The blank is very stable if the injection delay and sample sparging times are constant (see Injection Delay Time section).

Peak Width. Using peak *area*, the oxidation efficiency was found to be independent of column temperature (between 650 and 800 °C) for the column B design (Table 1). In contrast, the peak *width* for the different compounds changed significantly with temperature (Figure 8 and Table 3). For any *one* compound, this change with temperature is expected based on the ideal gas law ($PV = nRT$). However, at a constant temperature, the variations in peak width for *different* compounds must be related to some intrinsic property of the compounds, i.e., their refractory nature (or oxidation rate). From Table 3, this effect is most clearly seen at 650 °C. EDTA gave the broadest peak of the various standards, indicating that it is the most refractory compound under our oxidation conditions. The oxidation rate for the seawater sample was slightly greater than that of EDTA.

(30) Buesseler, K. O.; Bauer, J. E.; Chen, R. F.; Eglington, T. I.; Gustafsson, O.; Landing, W.; Mopper, K.; Moran, S. B.; Santschi, P. H.; VernonClark, R.; Wells, M. L. *Mar. Chem.*, in press (special issue Colloids in Seawater).

(31) Pearson, K. *Philos. Mag.* **1901**, *2*, 559−572.

It has been proposed that compositional/structural variability within natural water dissolved organic matter will affect the rate at which it is oxidatively degraded.[32] We suggest that peak width may be used as a new tool to quantify the oxidative refractiveness of OC in natural waters. However, our preliminary work suggests that quantification of this potential tool will strongly depend on the stability of the instrumental run conditions, including column temperature, flow rate, system dead volume, system back pressure, and injection technique. It may be possible to factor out instrumental variability by relating sample peak widths to that of a standard compound, e.g., methanol, injected at regular intervals while a set of samples is run. In addition, the relative stability of the described HTC system, including the autoinjection capability, should facilitate the exploration of peak width as a new potential tool. These efforts are currently in progress.

(32) Lee, C.; Henrichs, S. M. *Mar. Chem.* **1993**, *41*, 105−120.
(33) Guo, L., Santschi, P. H. *Mar. Chem.*, in press (special issue Colloids in Seawater).

ACKNOWLEDGMENT

We thank J. E. Bauer, L. Guo, and P. H. Santschi for allowing us to use their DOC data from the colloid intercomparison study (Figure 7). We are also grateful to E. T. Peltzer and an anonymous reviewer for insightful comments on the manuscript. We thank E. T. Peltzer for assistance in calculating Pearson's major axis (Figure 7), and for the stimulating discussions during the development of this instrument. We also thank S. B. Bentjen for her skilled assistance in preparing the manuscript and figures. Financial support was provided by the Chemical Oceanography Program of the National Science Foundation (OCE-9315821).

Received for review April 16, 1996. Accepted June 25, 1996.[⊗]

AC960370Z

[⊗] Abstract published in *Advance ACS Abstracts,* August 1, 1996.